ORIGINAL PAPER

Tracking of human cells in mice

**Wiebke Schormann · Friedrich J. Hammersen · Marc Brulport · Matthias Hermes · Alexander Bauer ·
Claudia Rudolph · Markus Schug · Thomas Lehmann · Andreas Nussler · Hendrik Ungefroren · James Hutchinson ·
Fred Fändrich · Jörg Petersen · Karsten Wursthorn · Martin R. Burda · Oliver Brüstle · Kannan Krishnamurthi ·
Marc von Mach · Jan G. Hengstler**

Abstract Tracking and tracing of transplanted cells in mice is required in many fields of research. Examples are transplantation of stem cells into organs of mice to study their differentiation capacity and injection of tumor cells to examine metastatic behavior. In the present study we tested the lipid dye CM-DiI and red fluorescent nanoparticles Qdot655 for their applicability in tagging and tracing of human cells in mice. Labeling of different cell types, including MCF-7 human breast cancer cells, human cord blood derived cells, human NeoHep cells and human hepatopancreatic precursor cells, is technically easy and did not compromise further cell culture. After transplantation of CM-DiI or Qdot655 marked cells, red fluorescent structures could be detected already in unprocessed paraffin slices of the studied organs, namely liver, lung, pancreas, kidney, spleen and bone marrow. Next, we examined whether the red fluorescent structures represent the transplanted human cells. For this purpose, we established an in situ hybridization (ISH) technique that allows clear-cut differentiation between human and murine nuclei, based on simultaneous hybridization with human *alu* and mouse major satellite (*mms*) probes. We observed a high degree of coincidence between CM-DiI-marked cells and *alu* positive nuclei. However, also some *mms* positive cells contained CM-DiI, suggesting phagocytosis of the transplanted CM-DiI-marked cells. The degree of such CM-DiI-positive mouse cells depended on the cell type and route of administration. From a technical point of view it was important that

W. Schormann (✉) · F. J. Hammersen · M. Brulport ·
M. Hermes · A. Bauer · C. Rudolph · M. Schug ·
J. G. Hengstler (✉)
Leibniz Research Centre for Working Environment
and Human Factors at the University of Dortmund (IfADo),
Ardeystrasse 67, 44139 Dortmund, Germany
e-mail: schormann@ifado.de

J. G. Hengstler
e-mail: hengstler@ifado.de

T. Lehmann
TRM-Leipzig, University of Leipzig,
Philipp-Rosenthal-Straße 55, 04103 Leipzig, Germany

A. Nussler
TU Munich, Department of Traumatology,
Ismaningerstr. 22, 81675 Munich, Germany

H. Ungefroren · J. Hutchinson · F. Fändrich
Department of General and Thoracic Surgery,
University Hospital Schleswig-Holstein,
Campus Kiel, Kiel, Germany

J. Petersen · K. Wursthorn · M. R. Burda
Department of Internal Medicine,
University Hospital Hamburg-Eppendorf,
Martinistr. 52, 20246 Hamburg, Germany

O. Brüstle
Institute of Reconstructive Neurobiology,
University of Bonn, Life and Brain Center and Hertie Foundation,
Bonn, Germany

K. Krishnamurthi
Environmental Biotechnology Division,
National Environmental Engineering Research
Institute (NEERI), Nagpur, India

M. von Mach
II. Medical Department, University of Mainz,
Langenbeckstr. 1, 55131 Mainz, Germany

CM-DiI-positive structures in paraffin slices remained fluorescent also after ISH. In contrast, Qdot655 positive structures faded during further staining procedures. In conclusion, marking of cells with CM-DiI or Qdot655 prior to transplantation facilitates recovery of human cells, since a high fraction of positive structures in the host's tissue originate from the transplanted cells. However, CM-DiI or Qdot655 positive staining of individual cells in transplanted tissues is not sufficient to prove their human origin. Additional procedures, such as ISH with *alu*-probes, are essential, when characterizing individual cells.

Keywords Stem cell · Alu probe · In situ hybridization · Mouse major satellite · CM-DiI · Qdot655 · Hepatopancreatic precursor cells · MCF7

Introduction

Many fields of research require tracking of human cells in mice. For instance, analysis of the metastatic properties of human tumor cells in mice demands a clear-cut differentiation between the human and the host's cells (Voura et al. 2004; Chambers et al. 2002; Fidler 2003; Friedl and Wolf 2003; Hengstler et al. 2006; Schmidt et al. 2007; Tanner et al. 2006; Hausherr et al. 2006; Spangenberg et al. 2006). Recently, numerous groups have analyzed the fate and differentiation capacity of human stem cells after transplantation into mice (Hengstler et al. 2005; Aurich et al. 2007; Eberhardt et al. 2006; Ruhnke et al. 2005a, b; Beerheide et al. 2002). These studies usually aim at demonstrating that previously silent markers of differentiated cells become expressed in the transplanted stem cells. They require unambiguous identification of the transplanted human cells.

The lipid dye CM-DiI and red fluorescent nanoparticles (Qdot655) have been introduced for tagging and tracing of cells (Andrade et al. 1996; Garon et al. 2007; Brulport et al. 2007). Both dyes allow marking of cells without causing cytotoxicity. Marking with CM-DiI and Qdot655 is easy to perform and the bright fluorescence of both dyes allows detection even in tissues with high background fluorescence, such as liver. However, little systematic work has been done to examine to which degree the (CM-DiI or nanoparticle-positive) fluorescent structures in tissues really represent the transplanted cells. Therefore, we established in situ hybridization techniques that allow differentiation between human and mouse nuclei and analyzed fluorescent structures in mouse tissues after transplantation of CM-DiI or nanoparticle marked cells. We report that both fluorescent dyes are useful for specific applications. However, pitfalls have to be anticipated to avoid misinterpretation.

Materials and methods

Cells and culture conditions

Isolation of human adherently proliferating cord blood cells was done as previously described (Beerheide et al. 2002). Briefly, umbilical cord blood was collected with informed consent of the mothers and loaded onto Ficoll solution (Biochrom, Berlin, Germany). After a density gradient centrifugation ($450g$, room temperature, 25 min) the mononuclear cells (MNC) from the interface were collected and washed twice in phosphate-buffered saline (2.7 mM KCl, 1.5 mM KH_2PO_4, 140 mM NaCl and 6.4 mM $Na_2HPO_4 \cdot 12H_2O$, PBS). The cells were plated in 25 cm^2 tissue flasks (Costar, Bodenheim, Germany). Adherent cells were cultured until single clones were visible. Adherently proliferating cord blood cells used for the transplantation experiments originated from a single clone and were cultured in 75 cm^2 tissue flasks (Greiner, Frickenhausen, Germany). William's Medium E supplemented with 10% fetal calf serum (Seraplus), 100 U/mL penicillin, 0.1 mg/mL streptomycin (all PAN Biotech, Aidenbach, Germany) and 100 nM dexamethasone (Sigma-Aldrich, Munich, Germany) was used as a cell culture medium for further passaging of cord blood cells. As soon as an initial clone resulted in a confluent culture on a 25 cm^2 tissue flask the cells were named as "passage no. 1". Cells from passage no. 1 were harvested by trypsinization, split onto five further 25 cm^2 tissue flasks resulting in passage no. 2, and so on. Twice a week cells were fed with fresh cell culture medium.

Generation of NeoHepatocyte (NeoHep) cells was performed as previously described by Ruhnke et al. (2005b). Briefly, mononuclear blood cells (MNCs) were isolated from buffy coats of healthy donors. MNCs were differentiated to NeoHep cells using a two-step procedure. In the first period of 6 days, MNCs were dedifferentiated to programmable cells of monocytic origin (PCMO) using RPMI1640 cell culture medium without phenol-red and L-glutamine (Cambrex, Baltimore, USA) supplemented with 10% human serum type AB0, 100 U/mL penicillin, 0.1 mg/mL streptomycin, 2 mM L-glutamine, 0.1 mM β-mercaptoethanol (all chemicals from Invitrogen, Carlsbad, USA), 5 ng/mL M-CSF and 0.4 ng/mL IL-3 (both R&D Systems, Wiesbaden-Nordenstedt, Germany). In order to generate NeoHep cells the PCMOs were cultured for a period of 12 days using a differentiation medium containing the same supplements as the dedifferentiation medium, but 3 ng/mL fibroblast growth factor-4 (FGF-4) (R&D Systems, Wiesbaden-Nordenstedt, Germany) instead of macrophage-colony stimulating factor (M-CSF) and interleukin-3 (IL-3) and no human serum type AB0, but 10% fetal calf serum (FCS). PCMOs and NeoHeps were both cultured in 75 cm^2 tissue

flasks (Sarstedt, Nümbrecht, Germany). Cell culture medium was exchanged in intervals of 2 days.

Native and immortalized nestin-positive hepatopancreatic precursor cells were obtained from Dr. Henryk Zulewski, University Hospital of Basel, Switzerland. Cells were cultured in RPMI1640 cell culture medium supplemented with 10% Seraplus, 100 U/mL, penicillin, 0.1 mg/mL streptomycin (all PAN Biotech, Aidenbach, Germany), 1 mM sodium pyruvate (Sigma-Aldrich, Munich, Germany), 50 µM β-mercaptoethanol, 10 mM HEPES (both Carl-Roth, Karlsruhe, Germany), 20 ng/mL basic fibroblast growth factor (bFGF) and 20 ng/mL epidermal growth factor (EGF) (both PAN Biotech, Aidenbach, Germany). Cells were cultured in 75 cm^2 tissue flasks (Greiner, Frickenhausen, Germany) and fed twice a week with fresh cell culture medium.

Mesenchymal bone marrow cells were obtained from Osiris (Osiris Therapeutics, Baltimore, USA), whereas primary human hepatocytes were a kind gift from Prof. Andreas Nüssler, Fresenius Biotech, Germany. The same cell culture medium used for adherently proliferating cord blood cells was also applied to culture mesenchymal bone marrow-derived stem cells and primary human hepatocytes.

All cells were cultured in an incubator with a humidified atmosphere at 37°C and 5% CO$_2$. For passaging of cord blood cells, mesenchymal bone marrow stem cells and hepatopancreatic precursor cells, the culture medium supernatant was removed and the cell monolayer was washed twice with PBS. Then 2.5 mL of 0.05% trypsin/0.02% EDTA (PAN Biotech, Aidenbach, Germany) was added to a 75 cm^2 tissue flask and incubated at 37°C for up to 5 min. Subsequently, incubation with trypsin was stopped by adding 10 mL of cell culture medium containing fetal calf serum to the tissue flask.

The MCF-7 breast carcinoma cell line was obtained from American Type Culture Collection (ATCC) and cultured at 37°C in humidified air atmosphere with 5% CO$_2$. Dulbecco`s Modified Eagle`s Medium (DMEM)/10% fetal calf serum (FCS) was used as growth medium (media and standard cell culture reagents were purchased from PAN Biotech, Aidenbach, Germany).

Marking of cells with CM-DiI

A stock solution of 1 mg/mL CM-DiI (Molecular Probes) was prepared in dimethyl sulfoxide (DMSO) and stored at 20°C. For marking of cells, the stock solution was diluted in cell culture medium to achieve a final concentration of 10 µg/mL. One million cells were suspended per mL and incubated for 30 min at 37°C, whereby cells were gently resuspended every 5 min. Afterwards, cells were washed twice in PBS (centrifugation for 10 min at 400g at room temperature) and resuspended in cell culture medium at 750,000 cells per 100 µL. The immunofluorescence of CM-DiI was investigated by means of a fluorescence microscope (BX41; Olympus, Japan) at an excitation wavelength of 543 nm (red Cy3 immunofluorescence).

Transplantation into NOD/SCID mice

(i) About 8–12 weeks old, non-obese diabetic/severe combined immune deficiency (NOD/SCID) male mice were used. The mice were anesthetized with 61.5 mg/kg ketamine (Ratiopharm) and 2.3 mg/kg xylazine hydrochloride (Bayer), whereby ketamine and xylazine were freshly diluted in 0.9% NaCl for each experiment. After disinfection with 70% ethanol and opening of the peritoneal cavity 750,000 cells suspended in 100 µL of cell culture medium were directly injected into the parenchyma of the left liver lobe. Injection was performed slowly over a period of 40–60 s. Successful injection was accompanied by a temporary pale color of the injected liver lobe. The cell suspension was kept on ice and heated to approximately 37°C immediately before injection. The muscular layer and the skin were closed by two sutures. After the time intervals given in the "Results" section mice were killed by neck dislocation. The peritoneal cavity was immediately opened, the complete left liver lobe was removed and fixed in 4% buffered formalin for 5–7 days. In order to remove erythrocytes, livers of some mice were perfused before removing the left liver lobe. For this purpose, the mice were anesthetized with 60 mg/kg pentobarbital, i.p., followed by cannulation of the lower vena cava, perfusion with approximately 10 mL PBS (heated to 37°C) at a flow rate of 10 mL/min followed by 50 mL 4% buffered formalin, also at a flow rate of 10 mL/min. After perfusion, the left liver lobe was removed and stored in 4% buffered formalin for 5–7 days.

(ii) For tail vein injection, the MCF-7 cells were harvested with trypsin and 5×10^6 cells were marked with Qdot655 in accordance with the manufacturer's protocol. A total of 10^6 cells were suspended in 100 µL phosphate-buffered saline (PBS) and injected i.v. by tail vein in CD1 nu/nu ($n = 5$; Charles River, Sulzfeld). The mice were killed 6 h after injection and the organs were fixed in formalin and embedded in paraffin. Slices were prepared and all single cells marked with Qdot655 as well as the marked cell clusters were counted.

(iii) For intrapancreatic transplantation, the mice were anesthetized and prepared as described above. After opening of the peritoneal cavity, 500,000 hepatopancreatic precursor cells suspended in 100 µL PBS were directly injected with a syringe (Micro-Fine, U-100, 29G, Becton Dickinson, USA) into the parenchyma of the
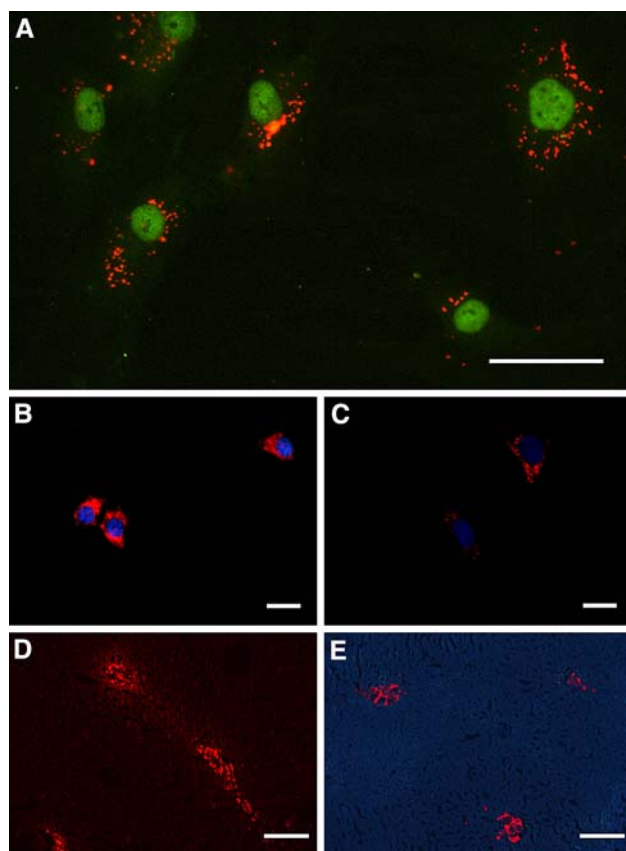
Fig. 1 Tagging of cells with the lipid dye CM-DiI and with red fluorescent nanoparticles (Qdot655). **a** Cultured cord blood cells tagged with Qdot655 after alu- in situ hybridization. Cultured cord blood cells tagged with CM-DiI (**b**) or with Qdot655 (**c**). After injection into mouse liver, red fluorescent structures can be identified already in unprocessed paraffin slices of the injected tissue. Human cord blood derived cells were tagged with CM-DiI (**d**) or with Qdot655 (**e**), injected into the left liver lobes of NOD/SCID mice and analyzed 12 h after injection. The *scale bar* is 50 μm in (**a**), 20 μm in (**b**, **c**) and 100 μm in (**d**)

Fig. 2 Red fluorescent structures in unprocessed paraffin slices of lung tissue 6 h after injection of Qdot655-tagged MCF-7 human breast cancer cells into the tail vein of CD1 nu/nu mice. The *scale bar* is 100 μm

Table 1 Red fluorescent structures in paraffin slices of various organs 6 h after injection of 1 million Qdot655-tagged MCF-7 cells into the tail vein of mice

Organ	No. of red fluorescent structures[a]
Blood	0.25 ± 0.23
Bone marrow	3.30 ± 1.49
Kidney	0.20 ± 0.17
Liver	4.30 ± 2.16
Spleen	0.40 ± 0.30
Heart	0.00 ± 0.00
Small intestine	0.00 ± 0.00
Lung	4.44 ± 1.27

Most red fluorescent structures were observed in lung, liver and bone marrow, whereas heart and small intestine were free of nanoparticles

[a] Mean values and standard error of five slices

pancreatic organ. Successful injection was accompanied by an edematous swelling of the whole pancreas. After the time intervals given in the "Results" section, the mice were killed by neck dislocation. The peritoneal cavity was immediately opened and the complete pancreatic organ was removed and fixation was performed as described above for the liver experiments.

(iv) For intracardiac transplantation, the mice were anesthetized as described above and after disinfection with 70% ethanol the skin of the ventral chest was opened by a midline incision. The muscles were cut in order to expose the ribs close to the pericardium, which allowed locating the beating heart. A total of 500,000 hepatopancreatic precursor cells suspended in 100 μL PBS were directly injected with a syringe (Micro-Fine, U-100, 29G, Becton Dickinson, USA) into the beating heart without opening the chest. To avoid an injection of the cells into the heart ventricles, a successful injection was controlled by aspiration. When no blood could be a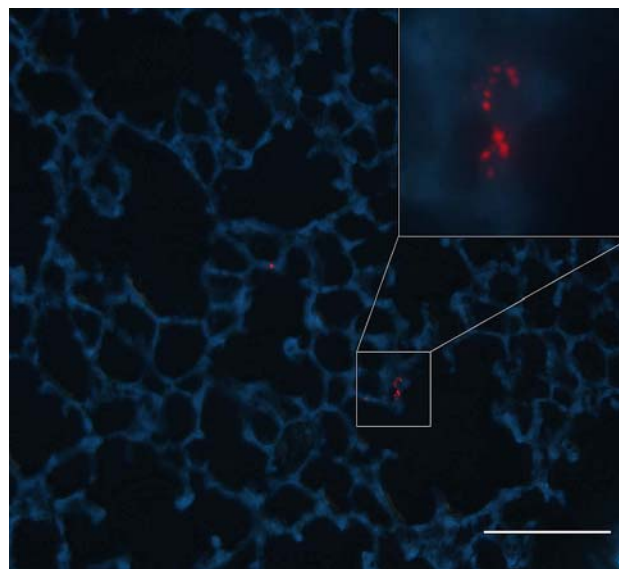spirated after drawing back the syringe piston, one-third of the cell suspension was injected into the heart muscle. This procedure was repeated two times in order to transplant the total amount of 100 μL of the cell suspension. After the time intervals given in the "Results" section, the mice were killed by neck dislocation. The chest was immediately opened the heart was removed and fixation was performed as described above for the liver experiments.

In situ hybridization with *alu*- and mouse major satellite probes

Sections were deparaffinized in xylene and rehydrated in graded ethanol series. The epitope retrieval was performed

Fig. 3 Mouse major satellite (mms) DNA and human alu sequences were detected by in situ hybridization. Murine liver from non-transplanted animals (**a**) and human liver (**c**) were incubated simultaneously with alu probe (*green*) and mms probe (*pink*) to demonstrate specific hybridization to the respective DNA sequences without cross hybridization. **b** Nuclear DAPI staining merged with the mms signal in (**a**). **d** Nuclear DAPI staining merged with the alu signal in (**c**). The *scale bar* is 50 μm
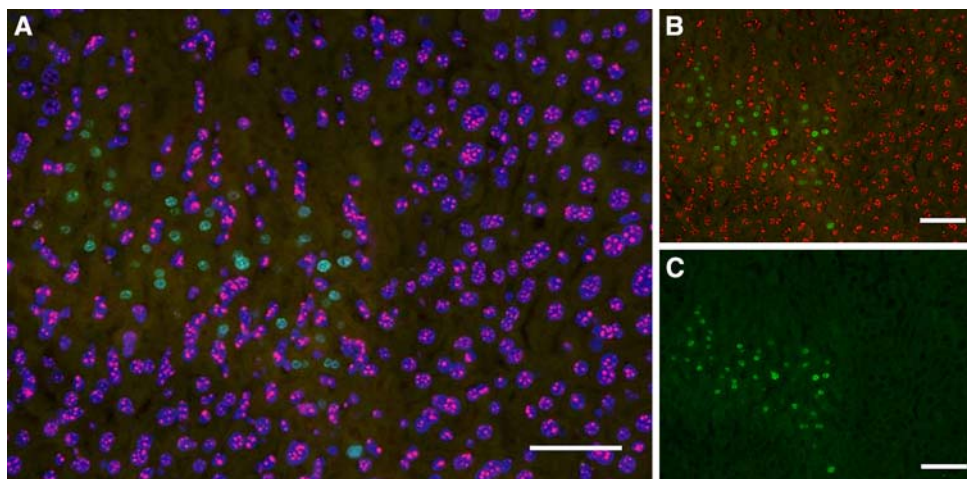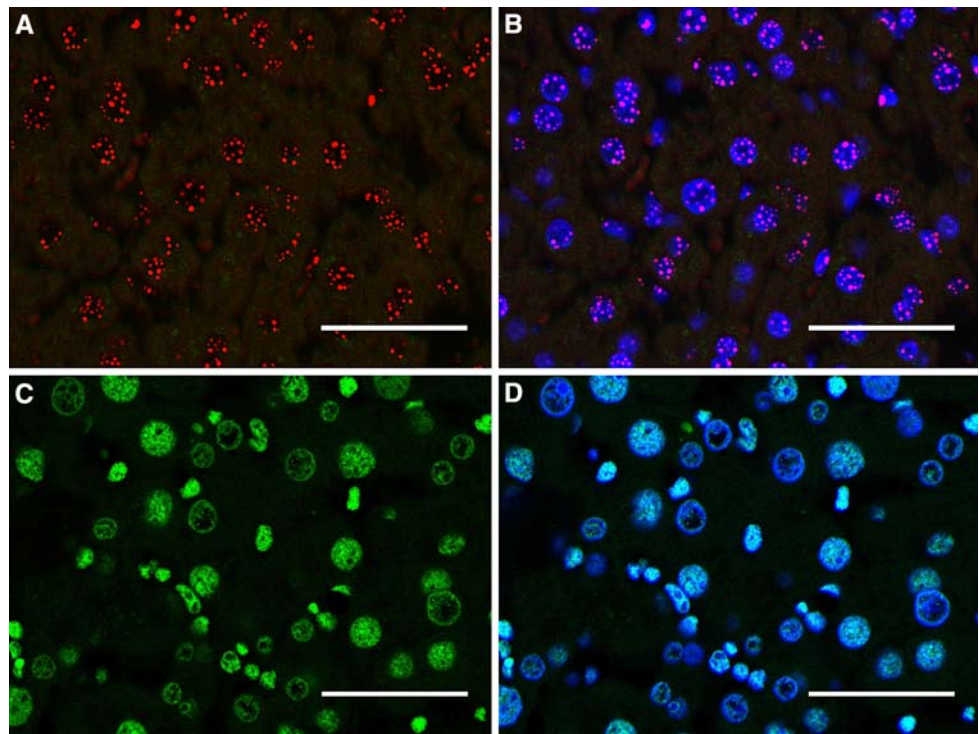

Fig. 4 Identification of human hepatocytes after transplantation into the left liver lobe of a NOD/SCID mouse. Slides were incubated with both, alu probe (*green fluorescence*) and mouse major satellite (mms) probe (*pink dots*). A total of 750,000 human hepatocytes were injected into the left liver lobe of an NOD/SCID mouse. Analysis was performed 12 h after injection. In situ hybridization clearly differentiates between human and mouse nuclei. **a** Merged signals of alu (*green*), mms (*pink*) and nuclear DAPI staining (*blue*). **b** *Green and pink fluorescence* without DAPI. **c** *Green fluorescence* only. The *scale bar* is 50 μm

using 0.01 M citrate buffer (citric acid, Carl-Roth, Karslruhe, Germany), pH 6.0, in a microwave oven. After cooling down, fluorescein-labeled *alu*-probe (BioGenex, San Ramon, CA, USA) and DIG (digoxigenin)-labeled major mouse satellite DNA were added simultaneously to the tissue slides, covered with coverslips and sealed with rubber cement. The sections were denaturated in a hybridizer (DakoCytomation, Denmark) at 95°C for 10 min followed by hybridization at 30°C overnight. The rubber cement and

the coverslips were removed and the sections were washed stringently. The stringent washing procedure was carried out using SSC buffer (saline sodium citrate) with 0.1% sodium dodecyl sulphate (SDS): 2× SSC/0.1% SDS for 2 × 5 min at room temperature, 0.1× SSC for 10 min at 40°C and 2× SSC/0.1% SDS for 5 min at room temperature. Unspecific binding sites were blocked with 3% bovine serum albumin (BSA)/1× PBS/0.1%Tween 20 for 1 h at room temperature, followed by an avidin-biotin-block

(Vector Lab., Burlingame, USA, SP-2001) as described by the manufacturer's protocol. The human probe detection was achieved using a biotinylated anti-fluorescein antibody (Vector Lab, Burlingame, USA, BA-0601; dilution 1: 100), followed by Streptavidin-Cy2 (Jackson ImmunoResearch Baltimore, MD; 016-220-084; dilution 1:100). The mouse-specific probe was visualized by using Cy3-conjugated secondary antibody against DIG (Jackson ImmunoResearch Baltimore, MD; 200-162-156; dilution 1: 250). After each antibody incubation, the slides were washed three times with PBS (pH 7.4). Afterwards, the nuclei were stained with 2.35 µg/mL 4′,6-diamidino-2-phenylindole (DAPI, Invitrogen, USA) for 5 min, followed by three washing steps in PBS for 5 min each. The immunofluorescence was investigated by means of a fluorescence microscope (BX41; Olympus) at an excitation wavelength of 543 nm (red Cy3 immunofluorescence) and 488 nm (yellow-green Cy2 immunofluorescence).

Results

Recovery of CM-DiI- and nanoparticle-marked human cells in mouse tissues

Both, the lipid dye CM-DiI and nanoparticles (Qdot655) allowed an efficient marking of human cells in vitro (Fig. 1). Qdot655 led to small, red fluorescent spots in the cytoplasm (Fig. 1a, c), whereas CM-DiI caused a diffuse cytoplasmic staining (Fig. 1b). After staining with CM-DiI or Qdot655, cells could be further cultivated in vitro. Marking with CM-DiI and Qdot655 was performed with MCF-7 human breast cancer cells (Fig. 2), human cord blood cells (Brulport et al. 2007), human hepatocytes, hepatopancreatic precursor cells (Eberhardt et al. 2006) and human blood monocyte-derived cells (Ruhnke et al. 2005a, b) showing that different cell types can be stained with similar efficiency.

In a next step, we transplanted CM-DiI and Qdot655-marked human cells into NOD/SCID mice. After injection of 7.5×10^5 CM-DiI or Qdot655-marked cells into the left liver lobes of NOD/SCID mice, we observed relatively large red fluorescent regions up to 2 months after transplantation, the longest time period analyzed in this study (CM-DiI, Fig. 1d; Qdot655: Fig. 1e). These red fluorescent structures could already be seen in unprocessed paraffin. Three mice each were analyzed 4, 12 and 24 h, and 3 weeks and 2 months after injection of human cord blood cells and 10 mice were mock-transplanted. Similar structures as shown in Fig. 1d and e were observed in all transplanted animals, but not in mock transplanted mice. After transplantation of cells into the left liver lobe, red fluorescent structures were also observed in lung tissue (Supplemental Figure 1). This
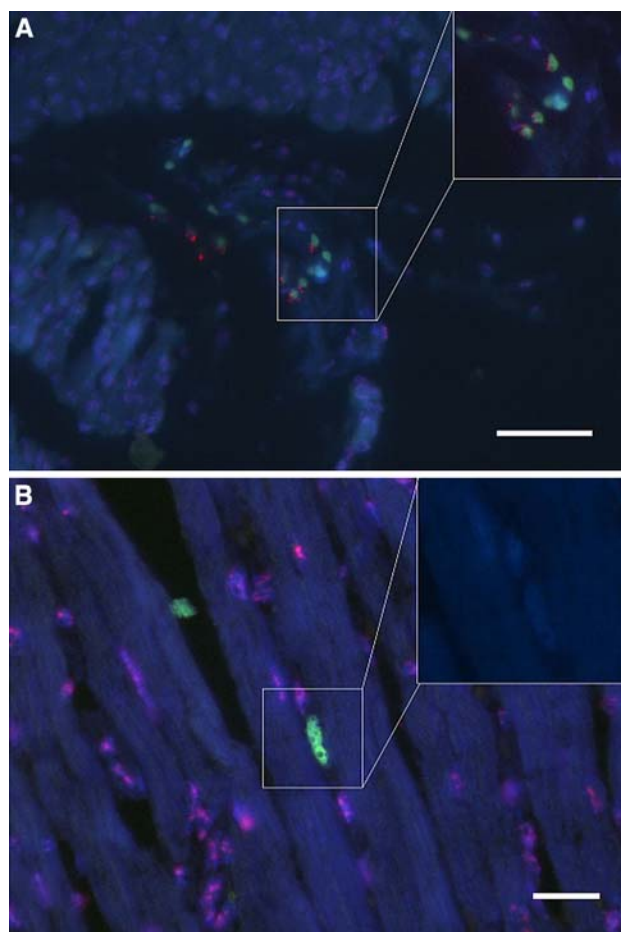

Fig. 5 Identification of human hepatopancreatic precursor cells after transplantation into the pancreas and heart muscle. Prior to the transplantation, the cells were labeled with nanoparticles and injected into the pancreas (**a**) of NOD/SCID mice. A total of 750,000 human cells were injected. Analysis was performed 12 h after injection. **b** Transplanted human cell in the heart muscle after alu- in situ hybridization. The *green signal* indicates an alu positive cell, the *pink spots* refer to mms and the *blue signals* show nuclear staining with DAPI. The *scale bar* is 50 µm in (**a**) and 20 µm in (**b**)

was not unexpected, since cells directly injected into the liver tissue are known to find their way into the venous system (Nussler et al. 2006). In order to study the applicability of Qdot655 for tracking of human tumor cells, we injected 10^6 nanoparticle (Qdot655)-marked MCF-7 cells into the tail vein of five mice. Qdot655-positive structures could be observed in unprocessed paraffin slices of not only lung tissue (Fig. 2), but also in liver, kidney, small intestine, bone marrow and blood (Table 1). In conclusion, red fluorescent structures could be reproducibly observed in mouse tissues after transplantation of several CM-DiI or Qdot655 marked cell types. An advantage of Qdot655 is their excellent contrast to background fluorescence. Excitation with 226 nm ultraviolet (UV) light and emission at >655 nm led to a dark blue background fluorescence of mouse tissues

allowing an easy and reliable differentiation of the red fluorescence of Qdot655.

Correlation of CM-DiI- and nanoparticle positive structures with human nuclei

Identification of CM-DiI- or nanoparticle (Qdot655)-positive structures does not automatically prove the human origin of these cells. One of several possibilities is that the fluorescence dye may be released from deteriorating cells and taken up by the surrounding mouse cells. In order to study whether CM-DiI and Qdot655-positive structures match human cells, we established an in situ hybridization technique that allows differentiation between mouse and human nuclei. Human nuclei are identified by *alu*-probes, resulting in green fluorescence of the complete nuclei (Fig. 3c). Mouse nuclei are visualized by hybridization with mouse major satellite (*mms*)-probes leading to red nuclear spots (Fig. 3a). Both probes (*alu* and *mms*) were simultaneously hybridized onto the same tissue slice. Combined *alu*- plus *mms*-hybridization allowed the unambiguous identification of human cells transplanted into mouse tissues. Examples are human hepatocytes after transplantation into mouse livers (Fig. 4a–c) and hepatopancreatic precursor cells after transplantation into the heart muscle (Fig. 5a) and pancreas (Fig. 5b). Thus, in situ hybridization with *alu*-plus *mms*-probes allows a clear-cut differentiation between human and mouse nuclei.

In a next step, we combined the analysis of CM-DiI fluorescence with *alu*- in situ hybridization in order to investigate the degree of coincidence of CM-DiI-marked cells and cells with *alu* positive human nuclei. Three weeks after transplantation of CM-DiI-marked human cells into the left liver lobe of NOD/SCID mice, we observed red fluorescent cells in liver tissue that also showed *alu* positive nuclei (Fig. 6a–d), obviously representing the initially transplanted human cells. Often CM-DiI-positive cell clusters were observed, whereby only a minority of CM-DiI-positive cells had *alu* positive nuclei (Fig. 6d). In situ hybridization with *mms*-probes demonstrated that CM-DiI can also occur in *mms* positive cells suggesting phagocytosis of the transplanted CM-DiI-marked human cells (Fig. 7). Similarly, we analyzed Qdot655-marked cells after in situ hybridization with *alu*-probes. However, Qdot655 faded and no longer showed red fluorescence after the in situ hybridization procedure.

Discussion

Tracking and tracing of transplanted cells in mice is required in many fields of research (Lewin et al. 2000; Voura et al. 2004; von Mach et al. 2004; Schiffer et al. 2003; Mohrmann et al. 2005; Trost et al. 2005; Eger et al. 2004). Tracking of individual cells can be achieved by three strategies: (1) expression of marker proteins, such as enhanced green fluorescent protein (EGFP) or β-galactosidase, (2) fluorescent dyes, exogenously loaded into the cells (Zhang et al. 2002) and (3) inorganic nanocrystals or nanoparticles (Koeppel et al. 2007; Jaiswal et al. 2004; Larson

Fig. 6 Combined analysis of CM-DiI fluorescence with alu-in situ hybridization. Red fluorescence was observed in cells with alu positive nuclei. However, in a smaller number of cells red fluorescence occurred also in alu-negative cells. The *insets* show the alu positive cells without green fluorescence. This demonstrates that the *green* alu-signal corresponds to the *blue* nuclear DAPI stain. **a–c** A total of 750,000 human NeoHep cells were injected into the left liver lobe of NOD/SCID mice. Analysis was performed 2 days after injection. **c** Mms-and alu- in situ hybridization was carried out. **d** A total of 750,000 human cord blood cells were injected into the left liver lobe of NOD/SCID mice. Analysis was performed 3 weeks after injection. The *scale bar* is 20 μm
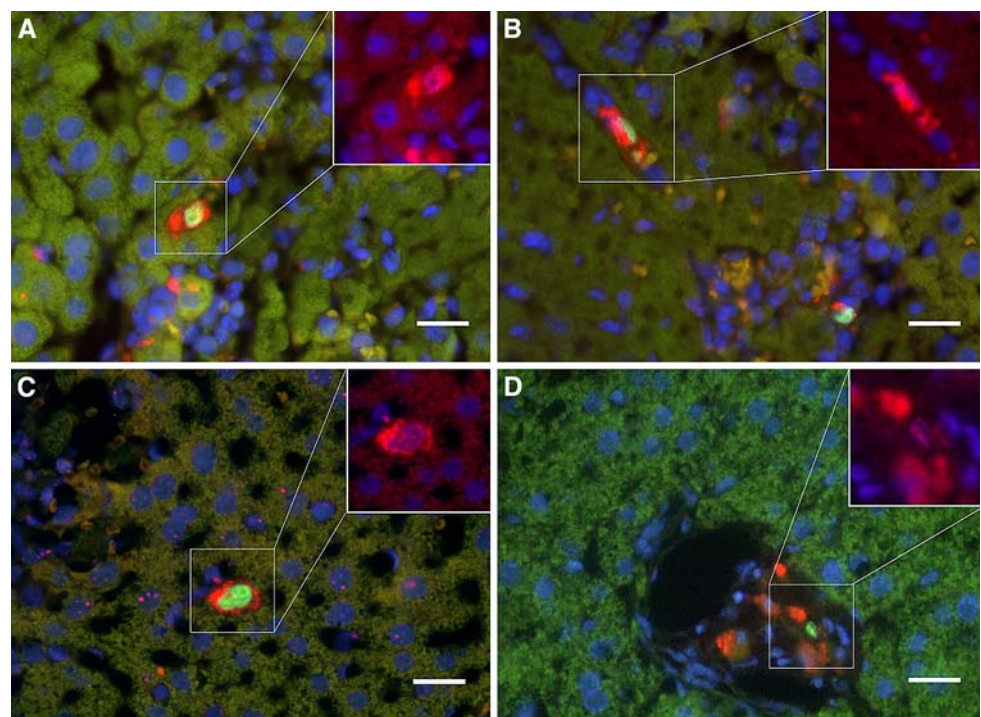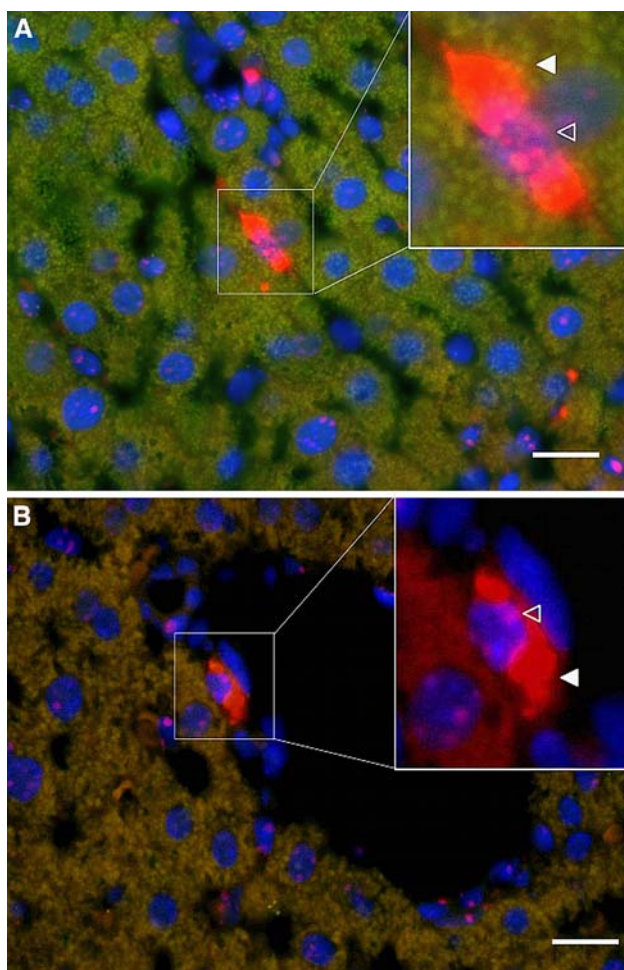
Fig. 7 *Red fluorescence* in the cytoplasm of a mouse-major-satellite positive nucleus. A total of 750,000 human cord blood cells were injected into the left liver lobe of NOD/SCID mice. Analysis was performed 3 weeks after injection. Merged signals of alu (*green*), mms (*pink*) and nuclear DAPI staining (*blue*). **a**, **b** *Open arrowheads* indicate nuclear mms-signals. *Closed arrowheads* show cytoplasm marked with CM-DiI. Obviously, both mms and CM-DiI are observed in the same cells. The *scale bar* is 20 μm

et al. 2003). These nanoparticles can be excited by a wide spectrum of excitation light and have the advantage of narrow emission spectra (Chan et al. 2002; Dabbousi et al. 1997; Jaiswal et al. 2003; Lim et al. 2003).

In the present study, we tested the lipid dye CM-DiI and red fluorescent nanoparticles Qdot655 for their applicability in tagging and tracing of human cells in mice. Labeling of cells with CM-DiI or Qdot655 is technically easy and can be performed within minutes. After transplantation of different human cell types with CM-DiI as well as Qdot655, we reproducibly observed red fluorescent structures in the transplanted mouse tissues. An obvious advantage of Qdot655 is their specific excitation/emission constellation. Excitation at 260 nm and emission at 655 nm result in a bright red fluorescence of Qdot655 and a dark blue back-

ground fluorescence of mouse tissues, which can be easily distinguished (for example: Fig. 2). This technique allows rapid screening of tissue slices. A disadvantage of Qdot655 is fading during additional staining procedures, such as in situ hybridization and immunostaining. Therefore, pictures of tissue slices containing Qdot655-marked cells have to be taken before and after staining in order to match the corresponding structures, which is laborious and time consuming. In contrast, CM-DiI-positive structures do not fade during in situ hybridization or immunostaining, which facilitates further analysis.

After transplantation of CM-DiI-marked cells into mice, we analyzed red fluorescent structures in mouse tissues by in situ hybridization using *alu*- and *mms*-probes, which allow differentiation between human and mouse nuclei. Human (*alu* positive) nuclei were reproducibly detected within CM-DiI-positive structures. However, not all CM-DiI-positive cells in mouse tissues were of human origin. The presence of CM-DiI fluorescent dye in some mouse (*mms*-positive) cells demonstrates the potential for transfer of fluorescent dye from grafted cells to host cells. The most probable scenario is that CM-DiI is released from deteriorating transplanted cells and taken up by the surrounding cells of the host. This is a critical source of misinterpretation, since the CM-DiI-positive mouse cells might be mistaken for transplanted cells. False positive results may be obtained when stem cells are transplanted into mice in order to analyze whether previously silent markers of mature cells become expressed. In order to avoid such problems, clear-cut results can be obtained by a combination of CM-DiI marking and *alu*-in situ hybridization. The green fluorescent nuclei in cells with CM-DiI-stained cytoplasm unambiguously identifies them as transplanted human cells (example: Fig. 6a). Additional combination with immunostaining for markers of mature cells (for instance, albumin in case of hepatocytes) allows further characterization of the grafted cells (Brulport et al. 2007).

In our experience, the degree of transfer of CM-DiI or Qdot655 from transplanted cells to the host's tissues depends on the cell type and route of administration. For instance, direct injection of human cord blood cells into liver tissue, conditions under which a relatively large fraction of transplanted cells deteriorate (Brulport et al. 2007), results in relatively high levels of dye transfer. In contrast, injection of MCF-7 cells into the tail vein followed by active extravasation into lung tissue resulted in lower levels of dye transfer.

In conclusion, we have validated CM-DiI and Qdot655 cell-marking techniques for tagging and tracing of human cells transplanted into mice. Both techniques allow identification of the transplanted cells. From a technical point of view it is easier to identify CM-DiI- or Qdot655-positive cells in tissue slices than performing in situ hybridization

for *alu* positive nuclei. However, false positive results may be caused by dye transfer to the host's cells. Therefore, validation with *alu*-in situ hybridization is required to confirm the human origin of CM-DiI or Qdot655-positive cells.

References

Andrade W, Seabrook TJ, Johnston MG, Hay JB (1996) The use of the lipophilic fluorochrome CM-DiI for tracking the migration of lymphocytes. J Immunol Methods 194:181–189

Aurich I, Mueller LP, Aurich H, Luetzkendorf J, Tisljar K, Dollinger M, Schormann W, Walldorf J, Hengstler J, Fleig WE, Christ B (2007) Functional integration of human mesenchymal stem cell-derived hepatocytes into mouse livers. Gut 56:405–415

Beerheide W, von Mach MA, Ringel M, Fleckenstein C, Schumann S, Renzing N, Hildebrandt A, Brenner W, Jensen O, Gebhard S, Reifenberg K, Bender J, Oesch F, Hengstler JG (2002) Downregulation of beta2-microglobulin in human cord blood somatic stem cells after transplantation into livers of SCID-mice: an escape mechanism of stem cells? Biochem Biophys Res Commun 294:1052–1063

Brulport M, Schormann W, Bauer A, Hermes M, Elsner C, Hammersen FJ, Beerheide W, Spitkovsky D, Härtig W, Nussler A, Horn LC, Edelmann J, Pelz-Ackermann O, Petersen J, Kamprad M, von Mach M, Lupp A, Zulewski H, Hengstler JG (2007) Fate of extrahepatic human stem and precursor cells after transplantation into mouse livers. Hepatology 46:861–870

Chambers AF, Groom AC, MacDonald IC (2002) Dissemination and growth of cancer cells in metastatic sites. Nat Rev Cancer 2:563–572

Chan WC, Maxwell DJ, Gao X, Bailey RE, Han M, Nie S (2002) Luminescent quantum dots for multiplexed biological detection and imaging. Curr Opin Biotechnol 13:40–46

Dabbousi BO, Rodriguez-Viejo J, Mikulec FV, Heine JR, Mattoussi H, Ober R, Jensen KF, Bawendi MG (1997) (CdSe) ZnS core-shell quantum dots: synthesis and characterization of a size series of highly luminescent nanocrystallites. J Phys Chem 101:9463–9475

Eberhardt M, Salmon P, von Mach MA, Hengstler JG, Brulport M, Linscheid P, Seboek D, Oberholzer J, Barbero A, Martin I, Muller B, Trono D, Zulewski H (2006) Multipotential nestin and Isl-1 positive mesenchymal stem cells isolated from human pancreatic islets. Biochem Biophys Res Commun 345:1167–1176

Eger K, Hermes M, Uhlemann K, Rodewald S, Ortwein J, Brulport M, Bauer A, Schormann W, Lupatsch F, Schiffer I, Heimerdinger C, Gebhard S, Spangenberg C, Pravitt D, Trost T, Zabel B, Tanner B, Krugel U, Franke H, Illes P, Madaj-Sterba P, Bockamp EO, Beckers T, Hengstler JG (2004) 4-Epidoxycycline: an alternative to doxycycline to control gene expression in conditional mouse models. Biochem Biophys Res Commun 323:979–986

Fidler IJ (2003) The pathogenesis of cancer metastasis: the 'seed and soil' hypothesis revisited. Nat Rev Cancer 3:453–458

Friedl P, Wolf K (2003) Tumour-cell invasion and migration: diversity and escape mechanisms. Nat Rev Cancer 3:362–374

Garon EB, Marcu L, Luong Q, Tcherniantchouk O, Crooks GM, Koeffler HP (2007) Quantum dot labeling and tracking of human leukemic, bone marrow and cord blood cells. Leuk Res 31:643–651

Hausherr CK, Schiffer IB, Gebhard S, Banic A, Tanner B, Kolbl H, Thoenes E, Beckers T, Spangenberg C, Prawitt D, Trost T, Zabel B, Oesch F, Hermes M, Hengstler JG (2006) Dephosphorylation of p-ERK1/2 in relation to tumor remission after HER-2 and Raf1 blocking therapy in a conditional mouse tumor model. Mol Carcinog 45:302–308

Hengstler JG, Brulport M, Schormann W, Bauer A, Hermes M, Nussler AK, Fandrich F, Ruhnke M, Ungefroren H, Griffin L, Bockamp E, Oesch F, von Mach M (2005) Generation of human hepatocytes by stem cell technology: definition of the hepatocyte. Expert Opin Drug Metab Toxicol 1:61–74

Hengstler JG, Bockamp EO, Hermes M, Brulport M, Bauer A, Schormann W, Schiffer IB, Hausherr C, Eshkind L, Antunes C, Franzen A, Krishnamurthi K, Lausch E, Lessig R, Chakrabarti T, Prawitt D, Zabel B, Spangenberg C (2006) Oncogene-blocking therapies: new insights from conditional mouse tumor models. Curr Cancer Drug Targets 6:603–612

Jaiswal JK, Mattoussi H, Mauro JM, Simon SM (2003) Long-term multiple color imaging of live cells using quantum dot bioconjugates. Nat Biotechnol 21:47–51

Jaiswal JK, Goldman ER, Mattoussi H, Simon SM (2004) Use of quantum dots for live cell imaging. Nat Methods 1:73–78

Koeppel F, Jaiswal JK, Simon SM (2007) Quantum dot-based sensor for improved detection of apoptotic cells. Nanomedicine 2:71–78

Larson DR, Zipfel WR, Williams RM, Clark SW, Bruchez MP, Wise FW, Webb WW (2003) Water-soluble quantum dots for multiphoton fluorescence imaging in vivo. Science 300:1434–1436

Lewin M, Carlesso N, Tung CH, Tang XW, Cory D, Scadden DT, Weissleder R (2000) Tat peptide-derivatized magnetic nanoparticles allow in vivo tracking and recovery of progenitor cells. Nat Biotechnol 18:410–414

Lim YT, Kim S, Nakayama A, Stott NE, Bawendi MG, Frangioni JV (2003) Selection of quantum dot wavelengths for biomedical assays and imaging. Mol Imaging 2:50–64

Mohrmann G, Hengstler JG, Hofmann TG, Endele SU, Lee B, Stelzer C, Zabel B, Brieger J, Hasenclever D, Tanner B, Sagemueller J, Sehouli J, Will H, Winterpacht A (2005) SPOC1, a novel PHD-finger protein: association with residual disease and survival in ovarian cancer. Int J Cancer 116:547–554

Nussler A, Konig S, Ott M, Sokal E, Christ B, Thasler W, Brulport M, Gabelein G, Schormann W, Schulze M, Ellis E, Kraemer M, Nocken F, Fleig W, Manns M, Strom SC, Hengstler JG (2006) Present status and perspectives of cell-based therapies for liver diseases. J Hepatol 45:144–159

Ruhnke M, Ungefroren H, Nussler A, Martin F, Brulport M, Schormann W, Hengstler JG, Klapper W, Ulrichs K, Hutchinson JA, Soria B, Parwaresch RM, Heeckt P, Kremer B, Fändrich F (2005a) Reprogramming of human peripheral blood monocytes into functional hepatocyte and pancreatic islet-like cells. Gastroenterology 128:1774–1786

Ruhnke M, Nussler AK, Ungefroren H, Hengstler JG, Kremer B, Hoeckh W, Gottwald T, Heeckt P, Fandrich F (2005b) Human monocyte-derived neohepatocytes: a promising alternative to primary human hepatocytes for autologous cell therapy. Transplantation 79:1097–1103

Schiffer IB, Gebhard S, Heimerdinger CK, Heling A, Hast J, Wollscheid U, Seliger B, Tanner B, Gilbert S, Beckers T, Baasner S, Brenner W, Spangenberg C, Prawitt D, Trost T, Schreiber WG, Zabel B, Thelen M, Lehr HA, Oesch F, Hengstler JG (2003) Switching off her-2/neu in a tetracycline-controlled mouse tumor model leads to apoptosis and tumor-size-dependent remission. Cancer Res 63:7221–7231

Schmidt M, Bremer E, Hasenclever D, Victor A, Gehrmann M, Steiner E, Schiffer IB, Gebhardt S, Lehr HA, Mahlke M, Hermes M, Mustea A, Tanner B, Koelbl H, Pilch H, Hengstler JG (2007) Role of the progesterone receptor for paclitaxel resistance in primary breast cancer. Br J Cancer 96:241–247

Spangenberg C, Lausch EU, Trost TM, Prawitt D, May A, Keppler R, Fees SA, Reutzel D, Bell C, Schmitt S, Schiffer IB, Weber A, Brenner W, Hermes M, Sahin U, Tureci O, Koelbl H, Hengstler JG, Zabel BU (2006) ERBB2-mediated transcriptional up-regulation of the alpha5beta1 integrin fibronectin receptor promotes

tumor cell survival under adverse conditions. Cancer Res 66:3715–3725

Tanner B, Hasenclever D, Stern K, Schormann W, Bezler M, Hermes M, Brulport M, Bauer A, Schiffer IB, Gebhard S, Schmidt M, Steiner E, Sehouli J, Edelmann J, Lauter J, Lessig R, Krishnamurthi K, Ullrich A, Hengstler JG (2006) ErbB-3 predicts survival in ovarian cancer. J Clin Oncol 24:4317–4323

Trost TM, Lausch EU, Fees SA, Schmitt S, Enklaar T, Reutzel D, Brixel LR, Schmidtke P, Maringer M, Schiffer IB, Heimerdinger CK, Hengstler JG, Fritz G, Bockamp EO, Prawitt D, Zabel BU, Spangenberg C (2005) Premature senescence is a primary fail-safe mechanism of ERBB2-driven tumorigenesis in breast carcinoma cells. Cancer Res 65:840–849

von Mach MA, Hengstler JG, Brulport M, Eberhardt M, Schormann W, Hermes M, Prawitt D, Zabel B, Grosche J, Reichenbach A, Muller B, Weilemann LS, Zulewski H (2004) In vitro cultured islet-derived progenitor cells of human origin express human albumin in severe combined immunodeficiency mouse liver in vivo. Stem Cells 22:1134–1141

Voura EB, Jaiswal JK, Mattoussi H, Simon SM (2004) Tracking metastatic tumor cell extravasation with quantum dot nanocrystals and fluorescence emission-scanning microscopy. Nat Med 10:993–998

Zhang J, Campbell RE, Ting AY, Tsien RY (2002) Creating new fluorescent probes for cell biology. Nat Rev Mol Cell Biol 3:906–918